

NBER WORKING PAPER SERIES

NEGATIVE INTEREST RATE POLICY AND THE YIELD CURVE

Jing Cynthia Wu  
Fan Dora Xia

Working Paper 25180  
<http://www.nber.org/papers/w25180>

NATIONAL BUREAU OF ECONOMIC RESEARCH  
1050 Massachusetts Avenue  
Cambridge, MA 02138  
October 2018

We thank Drew Creal, Felix Geiger, Jim Hamilton, Wolfgang Lemke, Monika Piazzesi, Eric Swanson, and seminar and conference participants at Northwestern Kellogg School of Management, 10th Annual Conference of the Society for Financial Econometrics, AFA Annual Meeting, the Federal Reserve Board's conference on "Developments in Empirical Monetary Economics," Barcelona GSE Summer Forum, 7th Term Structure Workshop at Bundesbank Bank, University of Oxford, Universitat Pompeu Fabra, European Central Bank, UCSD Rady School of Management, University of Illinois Urbana-Champaign, Texas A&M University, Tilburg University, Banque de France, Tinbergen Institute, University of Copenhagen, National Bank of Belgium, Universite Catholique de Louvain, Bank of Canada, and BIS Asian office for helpful suggestions. Cynthia Wu gratefully acknowledges financial support from the James S. Kemper Foundation Faculty Scholar at the University of Chicago Booth School of Business. This article was formerly titled "Time-Varying Lower Bound of Interest Rates in Europe." The views expressed herein are those of the authors and not necessarily the views of the BIS. Correspondence: [cynthia.wu@nd.edu](mailto:cynthia.wu@nd.edu), [dora.xia@bis.org](mailto:dora.xia@bis.org). The views expressed herein are those of the authors and do not necessarily reflect the views of the National Bureau of Economic Research.

NBER working papers are circulated for discussion and comment purposes. They have not been peer-reviewed or been subject to the review by the NBER Board of Directors that accompanies official NBER publications.

© 2018 by Jing Cynthia Wu and Fan Dora Xia. All rights reserved. Short sections of text, not to exceed two paragraphs, may be quoted without explicit permission provided that full credit, including © notice, is given to the source.

Negative Interest Rate Policy and the Yield Curve  
Jing Cynthia Wu and Fan Dora Xia  
NBER Working Paper No. 25180  
October 2018  
JEL No. E43,E52

**ABSTRACT**

We evaluate the implications of the ECB's negative interest rate policy (NIRP) on the yield curve. To capture various shapes of the short end of the yield curve induced by the NIRP, we introduce two policy indicators, which summarize the immediate and longer-horizon future monetary policy stances. We find the four NIRP events lowered the short term interest rate by the same amount. The impact is dampened at longer maturities for the first two event dates due to lack of forward guidance. In contrast, in the last two dates, forward guidance drives the largest effects in two years.

Jing Cynthia Wu  
Department of Economics  
3060 Jenkins Nanovic Hall  
University of Notre Dame  
Notre Dame, IN 46556  
and NBER  
cynthia.wu@nd.edu

Fan Dora Xia  
Bank for International Settlements  
Centralbahnpl. 2  
4002 Basel  
Switzerland  
dora.xia@bis.org

# 1 Introduction

The effective lower bound (ELB) of nominal interest rates is one of the most discussed economic issues of the past decade. The negative interest rate policy (NIRP) is among the latest additions to unconventional monetary policy toolkits, in the hopes of providing further stimulus to the economies that face the ELB. For example, in June 2017, the deposit rate of the Swiss National Bank was at a record low of  $-0.75\%$ , while the European Central Bank's (ECB) deposit facility rate was  $-0.4\%$ . The total volume of outstanding bonds with negative interest rates reached its peak at 15 trillion dollars in 2016.

As an emerging policy tool, it is important for policy makers and economists to understand its implications. The first question is what is the NIRP's impact on the yield curve? Second, what are economic agents' perceptions of this policy and how do they form expectations? Third, because the zero lower bound (ZLB) is no longer binding, the NIRP creates richer shapes for the short end of the yield curve. How do we accommodate them when we model the term structure of interest rates? Understanding these questions is important to European countries and Japan, which are currently implementing the NIRP. Such an understanding is also potentially important for the US economy, for which the NIRP remains a future option if large negative shocks hit the economy.

We propose a new shadow rate term structure model (SRTSM) to address these questions, and we focus on the Euro area. At the ELB, the short end of the yield curve displays three different shapes. The first case is flat, similar to what we see in the US data when the ZLB prevails but without the NIRP. Second, the yield curve could be downward sloping when agents expect future cuts of the policy rate due to the NIRP. Third, on some days, it is initially flat in the very short end and then downward sloping, implying market participants expect no immediate action from the central bank, but they think the overall future monetary policy is expansionary. To capture these shapes, we introduce two policy indicators: one for the immediate monetary policy stance, and the other for the future monetary policy stance at longer horizons. We model the discrete movement of the ECB's deposit facility rate at

the ELB with a simple and intuitive regime-switching model conditioning on the two policy indicators. Our model is able to capture the three different shapes at the short end of the yield curve that we see in the data. We then build the dynamics of the deposit rate into an SRTSM using the Black (1995) framework, where the short term interest rate is the maximum of the non-positive deposit rate and a shadow interest rate.

We use our model to extract the market's expectations on the NIRP. Overall, expectations of financial market participants from our model agree with economists' expectations from the Bloomberg survey. Importantly, our model has the advantage over the Bloomberg survey because we can extract the market's expectations further into the future, whereas the Bloomberg surveys are collected only one week before monetary policy meetings. We find the June 2014 and December 2015 cuts were expected the month before, and the September 2014 cut was entirely unanticipated. Most interestingly, the March 2016 cut was expected 4 months before the actual cut.

We then evaluate the NIRP's policy implications on the yield curve. For the four event dates, the ECB lowered the deposit rate by 10 basis points, which lowered the short end of the yield curve by the same amount. While the impact is dampened at longer maturities for the first two dates, the NIRP caused a humped shape change of the yield curve for the last two. We further decompose the NIRP into the rate cut itself and forward guidance. We find for the first two dates, the NIRP worked through the rate cut itself. For the later two dates, forward guidance became a significant part of the story, and it was the reason that drives the humped shape.

We assess the risk premium associated with the NIRP. We first measure it as the difference between the risk-neutral and real world conditional expectations. We find most of the time, the risk premium of the NIRP is positive or close to zero, which means agents typically associate a rate cut with an expansionary monetary policy. One exception is four months before the March 2016 cut, when the difference between the risk-neutral and physical expectations was almost -10 basis points. Our interpretation is that agents took a cut in

March 2016 as a sign of weak economic outlook. Relatedly, the NIRP drives a small but positive term premium on the 10-year yield.

We compare our model to several alternatives including several SRTSMs proposed in the literature and the Gaussian affine term structure model (GATSM). We find our new model performs the best in terms of higher likelihood and lower pricing errors. The existing models in the literature, on the other hand, do poorly.

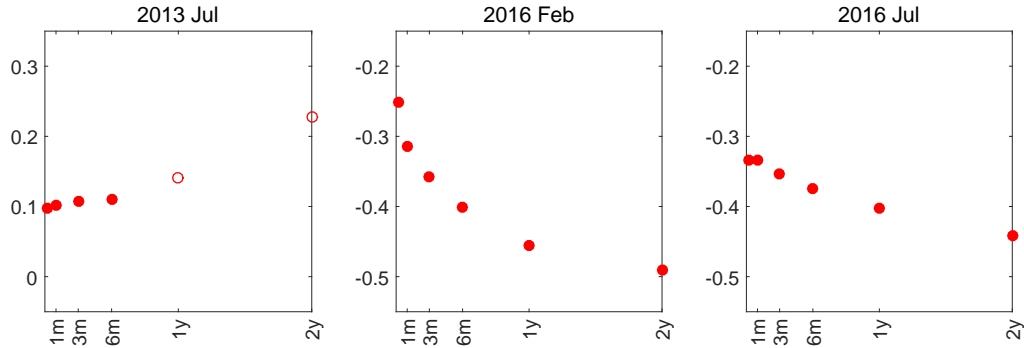
After a brief literature review, the rest of the paper proceeds as follows. [Section 2](#) models the dynamics of the deposit rate, and [Section 3](#) sets up the new SRTSM. [Section 4](#) discusses data, estimation, and estimates. [Section 5](#) examines markets' information on the NIRP, while [Section 6](#) assesses the NIRP's impact on the yield curve. [Section 7](#) compares our model to alternatives, and [Section 8](#) concludes.

**Literature** Earlier work has applied the SRTSM mostly to the Japanese and US yield curve. For example, Kim and Singleton (2012) and Ichiue and Ueno (2013) focus on Japan, whereas Krippner (2013), Christensen and Rudebusch (2014), Wu and Xia (2016), and Bauer and Rudebusch (2016) focus on the United States. These papers kept the lower bound at a constant level.

A few studies have worked on the new development in Europe, where the policy lower bound kept moving down to negative numbers after the NIRP. For example, Lemke and Vladu (2016) and Kortela (2016). However, none of these papers allow agents to be forward-looking in terms of the future movement of the policy rate, which is an important feature of our model. And this feature allows our model to fit the short end of the yield curve much better than the ones in the literature.

Our paper relates to the regime-switching literature, with the seminal paper by Hamilton (1989). Applications of this class of model in the term structure literature include Ang and Bekaert (2002), Bansal and Zhou (2002), and Dai et al. (2007). These papers allow the parameters of the dynamics to take several different values. In contrast, these parameters

Figure 1: Yield Curves



*Notes:* Yield curves in July 2013, February 2016, and July 2016. X-axis: maturity. Y-axis: yield in percentage points. Red solid dots correspond to ELB.

are constant in our model, and the deposit rate follows a regime switching process. Several papers are similar to ours in that sense, which model discrete movements of central banks' policy rates, for example, Rudebusch (1995), Piazzesi (2005), and Renne (2012). While Renne (2012) also uses a regime-switching process to model the discrete values of the ECB's policy rate, we allow a discrete policy rate only at the ELB. Otherwise, the state variables follow a Gaussian vector autoregression (VAR) as in the literature. The advantages of our model are twofold. First, it significantly reduces the state space for the regime-switching process. Second, when the ELB is not binding, our model is essentially the GATSM, which is the preferred model in the literature.

## 2 Modeling the short end of the yield curve with NIRP

The ELB introduces several new shapes for the short end of the yield curve. See the red solid dots in Figure 1. In July 2013, the front end of the yield curve was flat. This flatness was the basic pattern we see in the data when the US experienced the ZLB, and most efforts in the term structure literature for the ZLB focus on this feature.<sup>1</sup> However, the NIRP introduced additional patterns: in both February 2016 and July 2016, for example, the yield curves were

<sup>1</sup>See Christensen and Rudebusch (2014), Wu and Xia (2016), and Bauer and Rudebusch (2016), for example.

downward sloping, implying future decreases in the policy rate. Interestingly, the very short ends for the two months are different: in February 2016, an easing future monetary policy stance was expected throughout all horizons, whereas in July 2016, the very short end of the curve was flat, suggesting the cut would not happen in the next month.

We build a simple and intuitive model to capture these shapes in the short end of the yield curve in [Figure 1](#). We model the risk-neutral  $\mathbb{Q}$  dynamics of the deposit rate. When the ELB is binding, the forward rate at maturity  $n$  is approximately the  $\mathbb{Q}$  expectation of the deposit rate  $n$ -periods later. Hence the  $\mathbb{Q}$  dynamics dictate the shape of the yield curve. The physical dynamics take the same form with different parameter values.

We plot the dynamics of the deposit rate in [Figure 2](#), and summarize some basic data features: (1) the deposit rate is discrete and  $r_t^d \in \{0, -0.1, -0.2, -0.3, -0.4, \dots\}$  percentage point, and (2) the policy rate either stays where it was or moves down by 0.1%, which we formalize with the following dynamics<sup>2</sup>:

$$\begin{cases} \mathbb{Q}_t(r_{t+1}^d = r_t^d - 0.1) = \alpha_{1,t}^{\mathbb{Q}} \\ \mathbb{Q}_t(r_{t+1}^d = r_t^d) = 1 - \alpha_{1,t}^{\mathbb{Q}}, \end{cases} \quad (2.1)$$

where  $\mathbb{Q}_t$  is the conditional probability under the  $\mathbb{Q}$  measure.

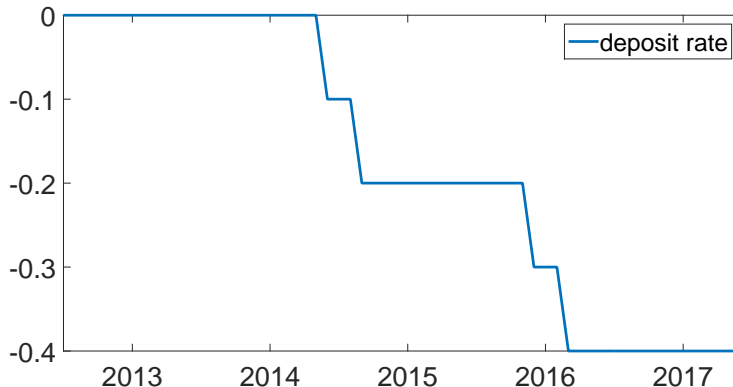
The simplest model with  $\alpha_{1,t}^{\mathbb{Q}} = \alpha_1^{\mathbb{Q}}$  implies one shape of yield curve. See the left panel of [Figure 3](#). This model is a slightly more flexible version of the existing model (see Wu and Xia (2016)), which imposes the restriction  $\alpha_1^{\mathbb{Q}} = 0$ . However, it cannot capture the other shapes in the data; see [Figure 1](#). In particular, it cannot capture both a flat curve (left panel) and a downward sloping curve (middle and right panels).

To separate these two shapes, we introduce a binary random variable  $\Delta_t$ , which captures agents' forecast of the ECB's next move.  $\Delta_t = 1$  indicates a high probability of a cut next period, whereas  $\Delta_t = 0$  implies monetary policy is more likely to stay put. We augment

---

<sup>2</sup>In the data, we have not observed the deposit rate move back up since the ELB. For a possible way to incorporate future upward movements, see Wu and Xia (2017).

Figure 2: Deposit rate



Notes: Sample spans from July 2012 to June 2017.

(2.1) with  $\Delta_t$ :

$$\mathbb{Q}_t(r_{t+1}^d = r_t^d - 0.1) = \mathbb{Q}(r_{t+1}^d = r_t^d - 0.1 | r_t^d, \Delta_t) = \alpha_{1,\Delta_t}^{\mathbb{Q}}, \quad (2.2)$$

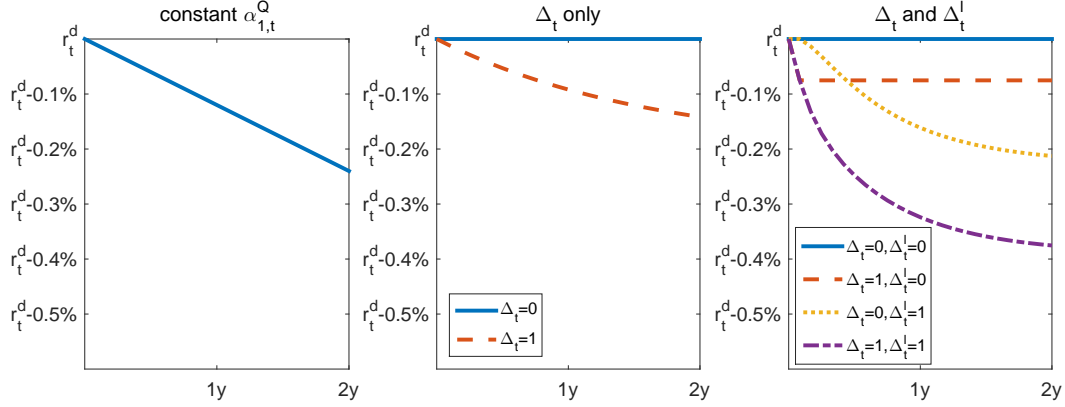
and  $\alpha_{1,\Delta_t=1}^{\mathbb{Q}} > \alpha_{1,\Delta_t=0}^{\mathbb{Q}}$  grants the interpretation of  $\Delta_t$ .

We model the dynamics of  $\Delta_t$  as a two-state Markov chain process:

$$\begin{cases} \mathbb{Q}_t(\Delta_{t+1} = 0 | \Delta_t = 0) = \alpha_{00,t}^{\mathbb{Q}} \\ \mathbb{Q}_t(\Delta_{t+1} = 1 | \Delta_t = 1) = \alpha_{11,t}^{\mathbb{Q}}. \end{cases} \quad (2.3)$$

If these probabilities are time invariant, that is,  $\alpha_{00,t}^{\mathbb{Q}} = \alpha_{00}^{\mathbb{Q}}$ ,  $\alpha_{11,t}^{\mathbb{Q}} = \alpha_{11}^{\mathbb{Q}}$ , this model implies two different shapes for the yield curve: one for  $\Delta_t = 1$  and one for  $\Delta_t = 0$ . The middle panel of Figure 3 provides an example of the two shapes. The blue line captures that the yield curve in the state  $\Delta_t = 0$  is flat, which corresponds to a long period of time in the data during which the short end of the yield curve is flat, such as the left panel of Figure 1. The red dashed line is for the state  $\Delta_t = 1$ , which sees a non-negligible probability of the deposit rate moving down. This can explain the shape in the middle panel of Figure 1. However, this model cannot capture the shape in the right panel of Figure 1. In this plot,

Figure 3: Expected paths of the deposit rate



*Notes:* The chart plots expected future paths of the deposit rate  $\mathbb{E}_t^Q(r_{t+h}^d | \Delta_t, \Delta_t^l, r_t^d)$ . The left panel corresponds to the case in which the transition probability for  $r_t^d$  is a constant:  $\alpha_1^Q = 0.1$ . The middle panel corresponds to the case in which the transition probability for  $r_t^d$  depends on  $\Delta_t$ :  $\alpha_{1,\Delta_t=0}^Q = 0$ ,  $\alpha_{1,\Delta_t=1}^Q = 0.1$ , and the constant transition probabilities for  $\Delta_t$  are  $\alpha_{00}^Q = 1$ ;  $\alpha_{11}^Q = 0.95$ . The right panel corresponds to the case in which the dynamics of  $r_t^d$  depends on both  $\Delta_t$  and  $\Delta_t^l$ . The parameters taken from the estimates in Table 1:  $\alpha_{1,\Delta_t=0}^Q = 0$ ;  $\alpha_{1,\Delta_t=1}^Q = 0.75$ ;  $\alpha_{00,\Delta_t^l=0}^Q = 1$ ;  $\alpha_{00,\Delta_t^l=1}^Q = 0.82$ ;  $\alpha_{11,\Delta_t^l=0}^Q = 0.0012$ ;  $\alpha_{11,\Delta_t^l=1}^Q = 0.75$ ;  $\alpha_{00}^{l,Q} = 1$ ;  $\alpha_{11}^{l,Q} = 0.88$ .

the market expects no immediate cut, but does expect a higher probability of a cut in future meetings.

To accommodate this possibility, we devise a separation between the immediate monetary policy stance  $\Delta_t$  and the longer-term monetary policy stance  $\Delta_t^l$ .  $\Delta_t^l = 1$  implies an easier monetary policy in longer horizons, whereas  $\Delta_t^l = 0$  implies a lower possibility for future cuts. We introduce this channel by allowing the dynamics of the state variable  $\Delta_t$  to depend on  $\Delta_t^l$ , and (2.3) becomes

$$\begin{cases} \mathbb{Q}_t(\Delta_{t+1} = 0 | \Delta_t = 0) = \mathbb{Q}(\Delta_{t+1} = 0 | \Delta_t = 0, \Delta_t^l) = \alpha_{00,\Delta_t^l}^Q \\ \mathbb{Q}_t(\Delta_{t+1} = 1 | \Delta_t = 1) = \mathbb{Q}(\Delta_{t+1} = 1 | \Delta_t = 1, \Delta_t^l) = \alpha_{11,\Delta_t^l}^Q. \end{cases} \quad (2.4)$$

We impose the identification restriction that  $\alpha_{00,\Delta_t^l=0}^Q > \alpha_{00,\Delta_t^l=1}^Q$ , and the basic intuition is if the economy is currently at the  $\Delta_t = 0$  state meaning no immediate cut, the probability

of a future cut for  $\Delta_t^l = 0$  is less than for  $\Delta_t^l = 1$ . We further assume

$$\begin{cases} \mathbb{Q}(\Delta_{t+1}^l = 0 | \Delta_t^l = 0) = \alpha_{00}^{l,Q} \\ \mathbb{Q}(\Delta_{t+1}^l = 1 | \Delta_t^l = 1) = \alpha_{11}^{l,Q}. \end{cases} \quad (2.5)$$

Our final model, constituting (2.2), (2.4), and (2.5), can capture various shapes of the yield curve; see the right panel of Figure 3.  $\Delta_t = 1$  corresponds to the case in which the market highly expects a cut in the next period (see the red dashed line and purple dash-dotted line), whereas  $\Delta_t = 0$  corresponds to no immediate cut in the coming month (see the blue solid line and yellow dotted line).  $\Delta_t^l = 1$  implies the market expects cuts not necessarily immediately but in the future (see the yellow dotted and purple dash-dotted lines). When  $\Delta_t^l = 0$ , agents do not anticipate much more policy actions past the next month (see blue solid and red dashed lines). The combination of  $\Delta_t = 0$  and  $\Delta_t^l = 1$  mimics the shape in the right panel of Figure 1.

### 3 A new shadow rate term structure model

This section incorporates the dynamics for the deposit rate introduced in Section 2 to an SRTSM, which we use to model the entire yield curve. Following Black (1995), the short-term interest rate  $r_t$  is the maximum function of the shadow rate  $s_t$  and a lower bound. The innovation of our paper is that the lower bound is time varying:

$$r_t = \max(s_t, \underline{r}_t). \quad (3.1)$$

Next, we describe how to model the lower bound and shadow rate, and then discuss how to price bonds.

### 3.1 Deposit rate and lower bound

The deposit rate is by definition the lower bound of the Euro OverNight Index Average (EONIA), and hence it naturally serves as the lower bound of the Overnight Index Swap (OIS) curve based on EONIA. We use a discrete-time model with month-end observations as in much of the term structure literature.<sup>3</sup> However, central banks do not meet at the end of the month. For our ELB sample, the ECB meets 8 to 12 times a year, at most once a month, and the meeting dates range from the 1<sup>st</sup> to the 27<sup>th</sup> day of the month. We will treat this calendar effect when we translate the deposit rate into the lower bound, because otherwise the date mismatch could be misleading. For example, suppose the meeting occurs on the 16<sup>th</sup> day of the next month for a 30-day month, and suppose agents predict the central bank will cut the deposit rate by 10 basis points with 100% chance. Then we will observe the one month forward rate reduce by 5 basis points, because we know nothing will happen between now and the 15<sup>th</sup>. If we do not treat the calendar effect, we will simply interpret the 5 basis point change in the forward rate as a 50% chance for a 10 basis point cut.

We incorporate this calendar effect when we model the lower bound. Suppose the number of days between the end of the current month  $t$  and the next meeting date is a fraction  $\gamma_t$  of the month from  $t$  to  $t + 1$ . When the ELB is binding, the monthly lower bound  $\underline{r}_t$  is the average of the overnight deposit rate for the month:

$$\begin{aligned}\underline{r}_t &\approx \gamma_t r_t^d + (1 - \gamma_t) \mathbb{E}_t^{\mathbb{Q}}(r_{t+1}^d) \\ &= r_t^d - (1 - \gamma_t) \alpha_{1, \Delta_t} \times 0.1.\end{aligned}\tag{3.2}$$

Note we only align the ECB's meeting schedule with our monthly data for the current month, that is, as of time  $t$ ,

$$\underline{r}_{t+n} = r_{t+n}^d, \quad \forall n \geq 1.\tag{3.3}$$

---

<sup>3</sup>For example, see Hamilton and Wu (2012b), Bauer et al. (2012), and Wright (2011).

We assume  $\underline{r}_t = 0$  if the economy is not at the ELB.

### 3.2 Shadow rate and factors

The shadow rate is an affine function of the latent yield factors, often labeled as “level,” “slope,” and “curvature”:

$$s_t = \delta_0 + \delta_1' X_t,$$

whose physical dynamics follow a first-order vector autoregression:

$$X_t = \mu + \rho X_{t-1} + \Sigma \varepsilon_t, \quad \varepsilon_t \sim N(0, I). \quad (3.4)$$

Similarly, the risk-neutral  $\mathbb{Q}$  dynamics are

$$X_t = \mu^{\mathbb{Q}} + \rho^{\mathbb{Q}} X_{t-1} + \Sigma \varepsilon_t^{\mathbb{Q}}, \quad \varepsilon_t^{\mathbb{Q}} \sim N(0, I).$$

### 3.3 Standard bond prices results

This section describes bond prices in general and how to price forward rate when the lower bound is a constant. All the results we present here are standard in the literature. The new results of our paper will be organized in [Subsection 3.4](#).

The no-arbitrage condition specifies that prices for zero-coupon bonds with different maturities are related by

$$P_{nt} = \mathbb{E}_t^{\mathbb{Q}}[\exp(-r_t) P_{n-1,t+1}].$$

The  $n$ -period yield relates to the price of the same asset as follows:

$$y_{nt} = -\frac{1}{n} \log(P_{nt}).$$

Following Wu and Xia (2016), we model forward rates rather than yields for the simplicity of the pricing formula. Define the one-period forward rate  $f_{nt}$  with maturity  $n$  as the return of carrying a zero-coupon bond from  $t + n$  to  $t + n + 1$  quoted at time  $t$ , which is a simple linear function of yields:

$$f_{nt} = (n + 1)y_{n+1,t} - ny_{nt}.$$

Therefore, modeling forward rates is equivalent to modeling yields. Note that  $f_{0t} = y_{1t} = r_t$ .

### 3.3.1 Forward rates with a constant lower bound

If the lower bound were a constant  $\underline{r}$ , Wu and Xia (2016) show the forward rate can be approximated by

$$f_{nt} \approx \underline{r} + \sigma_n^{\mathbb{Q}} g\left(\frac{a_n + b'_n X_t - \underline{r}}{\sigma_n^{\mathbb{Q}}}\right), \quad (3.5)$$

where the function  $g(\cdot)$  is

$$g(z) = z\Phi(z) + \phi(z), \quad (3.6)$$

and  $\Phi(\cdot)$  is the normal cumulative distribution function, while  $\phi(\cdot)$  is the normal probability density function.

Inside the  $g$  function,  $a_n + b'_n X_t$  is the  $n$ -period forward rate from the GATSM; see, for example, Ang and Piazzesi (2003) and Bauer et al. (2012). The coefficients  $a_n$  and  $b_n$  follow a set of difference equations whose solutions are

$$\begin{aligned} a_n &= \delta_0 + \delta'_1 \left( \sum_{j=0}^{n-1} (\rho^{\mathbb{Q}})^j \right) \mu^{\mathbb{Q}} - \frac{1}{2} \delta'_1 \left( \sum_{j=0}^{n-1} (\rho^{\mathbb{Q}})^j \right) \Sigma \Sigma' \left( \sum_{j=0}^{n-1} (\rho^{\mathbb{Q}})^j \right)' \delta_1 \\ b'_n &= \delta'_1 (\rho^{\mathbb{Q}})^n. \end{aligned}$$

In addition,  $(\sigma_n^Q)^2 \equiv \mathbb{V}_t^Q(s_{t+n})$  is the conditional variance of the future shadow rate, and

$$(\sigma_n^Q)^2 = \sum_{j=0}^{n-1} \delta_1' (\rho^Q)^j \Sigma \Sigma' (\rho^Q)^j \delta_1.$$

### 3.4 New bond prices results

Next, we derive the pricing formula in our new model. We begin by describing the distribution of the lower bound.

#### 3.4.1 Distribution of the lower bound

The probability distribution of interest for pricing purpose is the risk-neutral probability distribution of the lower bound  $n$  periods into the future  $\mathbb{Q}_t(r_{t+n})$ . It can be written as the sum of the joint distributions of the lower bound and  $\Delta$ ,  $\Delta^l$  states:

$$\mathbb{Q}_t(r_{t+n}) = \sum_{\Delta_{t+n}, \Delta_{t+n}^l} \mathbb{Q}_t(r_{t+n}, \Delta_{t+n}, \Delta_{t+n}^l). \quad (3.7)$$

The right-hand side can be written as

$$\begin{aligned} \mathbb{Q}_t(r_{t+n}, \Delta_{t+n}, \Delta_{t+n}^l) &= \sum_{r_{t+n-1}^d, \Delta_{t+n-1}, \Delta_{t+n-1}^l} \mathbb{Q}_t(r_{t+n-1}, \Delta_{t+n-1}, \Delta_{t+n-1}^l) \\ &\quad \times \mathbb{Q}_t(r_{t+n}, \Delta_{t+n}, \Delta_{t+n}^l | r_{t+n-1}, \Delta_{t+n-1}, \Delta_{t+n-1}^l), \end{aligned} \quad (3.8)$$

where the transition probability can be decomposed as follows

$$\begin{aligned}
& \mathbb{Q}_t(r_{t+n}, \Delta_{t+n}, \Delta_{t+n}^l | r_{t+n-1}, \Delta_{t+n-1}, \Delta_{t+n-1}^l) \\
= & \mathbb{Q}_t(r_{t+n} | \Delta_{t+n}, \Delta_{t+n}^l, r_{t+n-1}, \Delta_{t+n-1}, \Delta_{t+n-1}^l) \\
& \times \mathbb{Q}_t(\Delta_{t+n} | \Delta_{t+n}^l, r_{t+n-1}, \Delta_{t+n-1}, \Delta_{t+n-1}^l) \\
& \times \mathbb{Q}_t(\Delta_{t+n}^l | r_{t+n-1}, \Delta_{t+n-1}, \Delta_{t+n-1}^l) \\
= & \mathbb{Q}(r_{t+n} | r_{t+n-1}, \Delta_{t+n-1}) \mathbb{Q}(\Delta_{t+n} | \Delta_{t+n-1}, \Delta_{t+n-1}^l) \mathbb{Q}(\Delta_{t+n}^l | \Delta_{t+n-1}^l). \tag{3.9}
\end{aligned}$$

The last equal sign is based on the assumptions in (2.2), (2.4), and (2.5), and the assumption that the three variables are conditionally independent. The three terms in (3.9) are specified in (2.2), (2.4), and (2.5).

### 3.4.2 Forward rates in the new model

With the results in Section 3.4.1, the pricing formula in (3.5) becomes

$$f_{nt} \approx \sum_{r_{t+n}} \left( r_{t+n} + \sigma_n^{\mathbb{Q}} g \left( \frac{a_n + b'_n X_t - r_{t+n}}{\sigma_n^{\mathbb{Q}}} \right) \right) \mathbb{Q}_t(r_{t+n}), \tag{3.10}$$

where  $\mathbb{Q}(r_{t+n})$  is specified in (3.7). Derivations for the new pricing formula are in [Appendix A.1](#).

The forward rate in (3.10) differs from (3.5) due to the time-varying lower bound. The new pricing formula (3.10) prices in the uncertainty associated with the future dynamics of the lower bound. The forward rate is calculated as an average of forward rates given  $r_{t+n}$ , weighted by the risk-neutral probability distribution of  $r_{t+n}$ . If  $r_{t+n}$  were a constant, (3.10) would become (3.5).

The regime-switching dynamics of  $(r_t^d, \Delta_t, \Delta_t^l)$  preserve the analytical approximation for the pricing formula. Having an analytical approximation is crucial for the model to be tractable and have better numerical behavior. Dynamic term structure models are often

criticized for being difficult to estimate. For example, in the class of GATSMs, which is a special case of our model when  $\underline{r}_t \rightarrow -\infty$  and has analytical bond prices, a literature has been dedicated to improving the model’s performance.<sup>4</sup> If we had to compute bond prices numerically, the model would behave even worse.

## 4 Estimation

### 4.1 Data and estimation details

**Data** We model OIS rates on EONIA, and data is from Bloomberg. Our sample is monthly from July 2005 to June 2017. We date the ELB period when the deposit rate is less than or equal to zero starting from July 2012.

**Spread** The deposit rate is the floor for EONIA. In our model, they are the same for the ELB sample. However, in the data, the former is always lower than the latter. To capture this difference, we introduce a spread. The deposit rate is measured overnight. However, the overnight EONIA rate is very volatile due to some month-end effects. Therefore, we define the spread as the difference between the one-week EONIA-based OIS rate and the overnight deposit rate:  $sp_t = r_t^{week} - r_t^d$ . [Figure 4](#) plots the time-series dynamics of the one-week OIS rate and the overnight deposit rate in the top panel and their difference at the bottom to demonstrate a non-zero and time-varying spread.

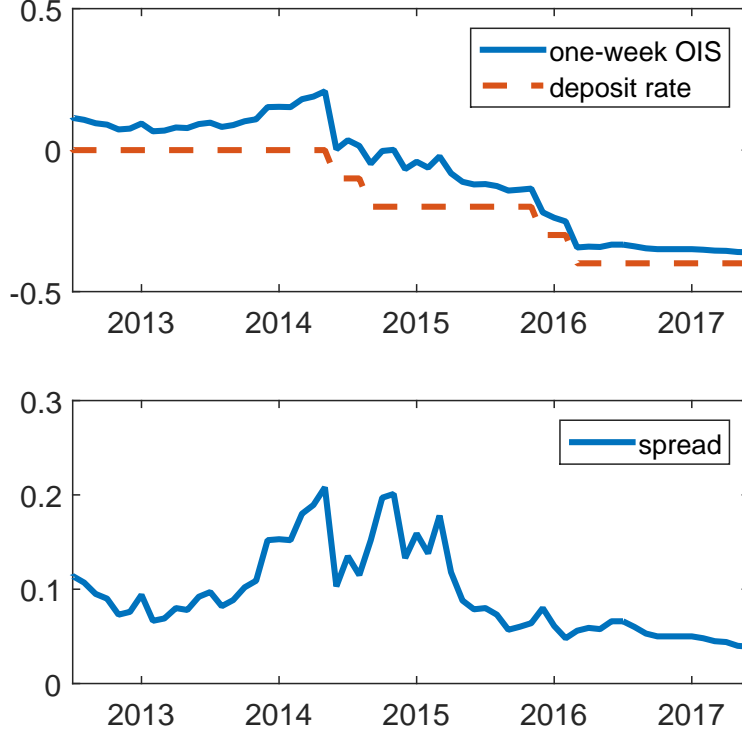
We assume the spread  $sp_t$  follows an AR(1) under the risk-neutral measure:

$$sp_t = \mu_{sp}^{\mathbb{Q}} + \rho_{sp}^{\mathbb{Q}} sp_{t-1} + e_t^{\mathbb{Q}}, \quad e_t^{\mathbb{Q}} \sim N(0, \sigma_{sp}^2). \quad (4.1)$$

---

<sup>4</sup>See Joslin et al. (2011), Christensen et al. (2011), Hamilton and Wu (2012b), Adrian et al. (2012), Creal and Wu (2015), and de Los Rios (2015).

Figure 4: Spread



Notes: Top panel: time-series dynamics of the one-week OIS rate in blue solid line and deposit rate in red dashed line; bottom panel: the spread defined as the difference between the two lines in the top panel. X-axis: time. Y-axis: interest rates in percentage points. Sample spans from July 2012 to June 2017.

This modifies the pricing formula in (3.10) to

$$f_{nt} \approx \sum_{r_{t+n}} \mathbb{Q}_t(r_{t+n}) \left( r_{t+n} + c_n + d_n sp_t + \tilde{\sigma}_n^{\mathbb{Q}} g \left( \frac{a_n + b'_n X_t - r_{t+n} - c_n - d_n sp_t}{\tilde{\sigma}_n^{\mathbb{Q}}} \right) \right) \quad (4.2)$$

where  $c_n = (\sum_{j=0}^{n-1} (\rho_{sp}^{\mathbb{Q}})^j) \mu_{sp}^{\mathbb{Q}}$ ,  $d_n = (\rho_{sp}^{\mathbb{Q}})^n$ ,  $(\tilde{\sigma}_n^{\mathbb{Q}})^2 = (\sigma_n^{\mathbb{Q}})^2 + (\sum_{j=0}^{n-1} (\rho_{sp}^{\mathbb{Q}})^{2j}) \sigma_{sp}^2$ . See Appendix A.2 for the derivation.

Combine (3.1) and (3.2), and add a spread,

$$r_t = \begin{cases} r_t^d - (1 - \gamma_t) \alpha_{1, \Delta_t}^{\mathbb{Q}} \times 0.1 + sp_t, & \text{for ELB} \\ s_t, & \text{otherwise.} \end{cases} \quad (4.3)$$

**Forward rates** We use OIS yields with the following maturities: three and six months, and one, two, three, five, six, seven, eight, nine, and ten years, and transform them into forward rates. We transform yields into forward rates  $f_{nmt}$ , defined as the return of a forward contract carrying a bond from  $t + n$  to  $t + n + m$ , as follows:

$$f_{nmt} = \frac{1}{m}[(n + m)y_{n+m,t} - ny_{nt}].$$

The forward rates we model include  $f_{3,3,t}$ ,  $f_{6,6,t}$ ,  $f_{12,12,t}$ ,  $f_{24,12,t}$ ,  $f_{60,12,t}$ ,  $f_{84,12,t}$ , and  $f_{108,12,t}$ .  $f_{nmt}$  relates to the forward rate in (4.2) with

$$f_{nmt} = \frac{1}{m}(f_{nt} + f_{n+1,t} + \dots + f_{n+m-1,t}). \quad (4.4)$$

There are a couple of advantages of modeling forwards rates over yields. First, forward rates require summing over fewer terms per (4.4). Second, forward rates do not involve the “max” operator, which is included in yields of any maturity. Having the “max” operator is problematic for any gradient-based numerical optimizer.

**State space form** The state variables  $X_t$ ,  $\Delta_t$ , and  $\Delta_t^l$  are latent, whereas  $r_t^d$  and  $sp_t$  are observed. Our SRTSM is a nonlinear state-space model. The transition equations include (3.4), and the P version of (2.2), (2.4), (2.5), and (4.1), where we assume the same process under the physical dynamics  $\mathbb{P}$  and risk-neutral dynamics  $\mathbb{Q}$  but with different parameters. The difference between them captures the risk premium.

Adding measurement errors to (4.3) and (4.4), the measurement equations are

$$r_t^o = r_t + \eta_t \quad (4.5)$$

$$f_{nmt}^o = f_{nmt} + \eta_{nmt}, \quad (4.6)$$

where the “o” superscript stands for observed data, and the measurement errors are i.i.d.

normal:  $\eta_t, \eta_{mnt} \sim N(0, \omega^2)$ .

**Normalization** The collection of parameters we estimate consists of four subsets: (1) parameters related to  $r_t^d, \Delta_t$ , and  $\Delta_t^l$ , including  $\alpha_{1,\Delta_t=0}, \alpha_{1,\Delta_t=1}, \alpha_{00,\Delta_t^l=0}, \alpha_{11,\Delta_t^l=0}, \alpha_{00,\Delta_t^l=1}, \alpha_{11,\Delta_t^l=1}, \alpha_{00}^l, \alpha_{11}^l$  and  $\alpha_{1,\Delta_t=0}^Q, \alpha_{1,\Delta_t=1}^Q, \alpha_{00,\Delta_t^l=0}^Q, \alpha_{11,\Delta_t^l=0}^Q, \alpha_{00,\Delta_t^l=1}^Q, \alpha_{11,\Delta_t^l=1}^Q, \alpha_{00}^{l,Q}, \alpha_{11}^{l,Q}$ . (2) parameters describing the dynamics of  $sp_t$ , including  $(\mu_{sp}, \mu_{sp}^Q, \rho_{sp}, \rho_{sp}^Q, \sigma_{sp})$ ; (3) parameters related to  $X_t$ , including  $(\mu, \mu^Q, \rho, \rho^Q, \Sigma, \delta_0, \delta_1)$ ; and (4) the parameter for pricing error:  $\omega$ . For identification, we impose  $\alpha_{1,\Delta_t=1}^Q > \alpha_{1,\Delta_t=0}^Q$  and  $\alpha_{00,\Delta_t^l=0}^Q > \alpha_{00,\Delta_t^l=1}^Q$ . The identifying restrictions on the group (3) are similar to Hamilton and Wu (2014): (i)  $\delta_1 = [1, 1, 1]'$ , (ii)  $\mu^Q = 0$ , (iii)  $\rho^Q$  is diagonal with eigenvalues in descending order, and (iv)  $\Sigma$  is lower triangular.

**Estimation** We estimate the model by maximum likelihood with the algorithm for regime-switching state space models of Kim (1994) and the extended Kalman filter. The details are in [Appendix B](#). In practice, we impose  $r_t^d \in \{0, -0.1, -0.2, -0.3, -0.4, \dots, -1\}$ , and therefore  $\mathbb{Q}(r_{t+1}^d = r_t^d - 0.1 | r_t^d = -1, \Delta_t) = 0$ .

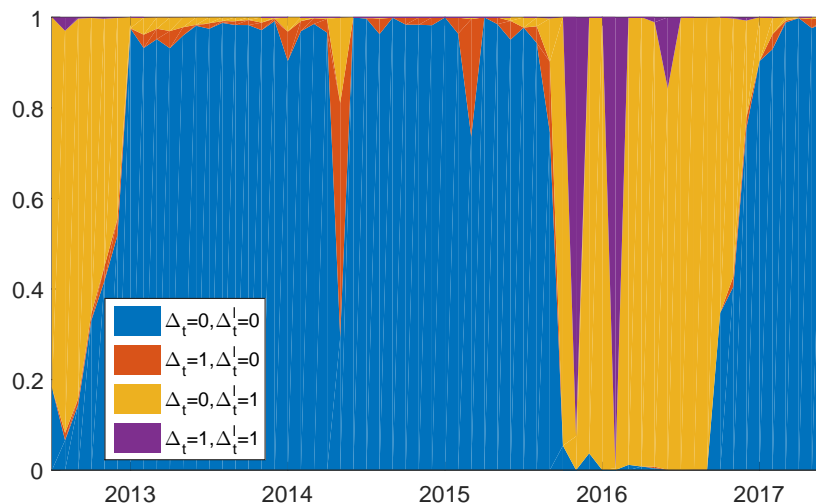
We report maximum likelihood estimates and robust standard errors (see Hamilton (1994)) in [Table 1](#). The eigenvalues of  $\rho, \rho^Q$  indicate the factors  $X_t$  are highly persistent under both measures. This finding is consistent with the term structure literature. Both  $\alpha_{1,\Delta_t=0}$  and  $\alpha_{1,\Delta_t=0}^Q$  are zero, which means that when  $\Delta_t = 0$ , agents do not expect the deposit rate to change in the next period. When  $\Delta_t = 1$ , the probability of the ECB cutting the deposit rate is much higher:  $\alpha_{1,\Delta_t=1} = 1$  under the physical measure, and  $\alpha_{1,\Delta_t=1}^Q = 0.75$  under the risk-neutral measure. The difference between the two measures reflects the risk premium. The  $\Delta_t = 0$  state is very persistent, with the probability of staying in this state  $(\alpha_{00,\Delta_t^l}, \alpha_{00,\Delta_t^l}^Q)$  being 95% or 100% when  $\Delta_t^l = 0$ . The numbers are lower when  $\Delta_t^l = 1$ , and they are 89% or 82%. By contrast, the  $\Delta_t = 1$  state is much less persistent. The spread  $sp_t$  follows a persistent autoregressive process under both measures. Other parameters are comparable to what we see in the literature.

Table 1: Maximum likelihood estimates

$\alpha_{1,\Delta_t=0}$	0.0000 (0.0000)			$\alpha_{1,\Delta_t=0}^Q$	0.0000 (0.0000)		
$\alpha_{1,\Delta_t=1}$	1.0000 (0.0000)			$\alpha_{1,\Delta_t=1}^Q$	0.7510 (0.1777)		
$\alpha_{00,\Delta'_i=0}$	0.9464 (0.0344)			$\alpha_{00,\Delta'_i=0}^Q$	1.0000 (0.0000)		
$\alpha_{11,\Delta'_i=0}$	0.0002 (0.0005)			$\alpha_{11,\Delta'_i=0}^Q$	0.0012 (0.0023)		
$\alpha_{00,\Delta'_i=1}$	0.8857 (0.0770)			$\alpha_{00,\Delta'_i=1}^Q$	0.8232 (0.0587)		
$\alpha_{11,\Delta'_i=1}$	0.0000 (0.0001)			$\alpha_{11,\Delta'_i=1}^Q$	0.7516 (0.1726)		
$\alpha_{00}^l$	0.9735 (0.0265)			$\alpha_{00}^{l,Q}$	1.0000 (0.0000)		
$\alpha_{11}^l$	0.9013 (0.0331)			$\alpha_{11}^{l,Q}$	0.8815 (0.0429)		
$1200\mu_{sp}$	0.0114 (0.0000)			$1200\mu_{sp}^Q$	0.0084 (0.0049)		
$\rho_{sp}$	0.8674 (0.0000)			$\rho_{sp}^Q$	0.9361 (0.0407)		
$1200\sigma_{sp}$	0.0786 (0.0045)						
$1200\mu$	-0.0272 (0.1385)	-1.2246 (1.2907)	0.9167 (1.2592)	$1200\mu^Q$	0	0	0
$\rho$	0.9932 (0.0250)	0.0265 (0.0177)	0.0228 (0.0181)	$\rho^Q$	0.9964 (0.0005)	0	0
	-0.1136 (0.2628)	0.4675 (1.3064)	-0.4494 (1.3295)		0	0.9293 (0.0032)	0
	0.0581 (0.2547)	0.3983 (1.2818)	1.3133 (1.3047)		0	0	0.9257 (0.0034)
$ eig(\rho) $	0.9875	0.8939	0.8939				
$\delta_0$	7.6098 (0.5368)						
$1200\Sigma$	0.5961 (0.0511)	0	0				
	-12.5099 (0.8773)	10.4538 (0.2589)	0				
	11.8193 (0.8712)	-10.3705 (0.2415)	0.1715 (0.0264)				
$1200\omega$	0.0235 (0.0000)						

Notes: Maximum likelihood estimates with quasi-maximum likelihood standard errors in parentheses. Sample: July 2005 to June 2017.

Figure 5: Filtered probabilities for different states



*Notes:* Areas with different colors correspond to the filtered probabilities of different states. From the bottom to top are: blue for  $\Delta_t = 0, \Delta_t^l = 0$ , red for  $\Delta_t = 1, \Delta_t^l = 0$ , yellow for  $\Delta_t = 0, \Delta_t^l = 1$ , and purple for  $\Delta_t = 1, \Delta_t^l = 1$ .

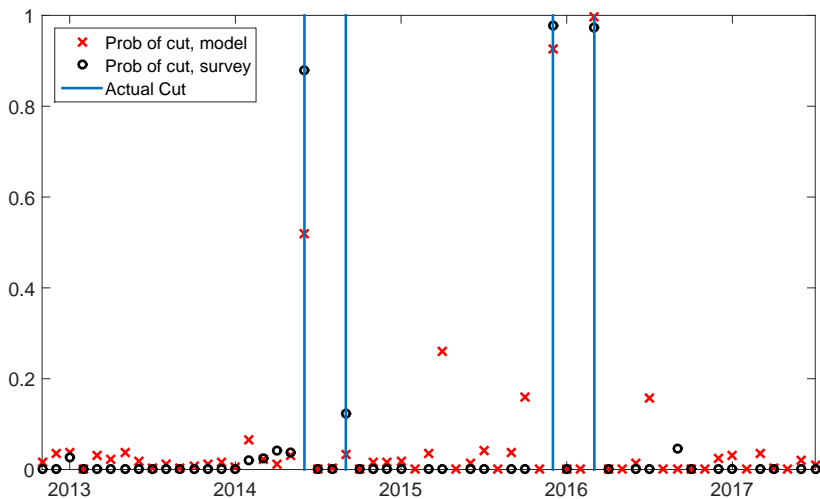
## 5 Markets' information on the NIRP

In this section, we extract the market's expectations on the NIRP from the yield curve using our SRTSM. We first filter out the probabilities for different policy states over time. Then we extract the model implied probability of a rate cut, and compare it with some survey data. Finally, we illustrate superior information contained in our model that is not available in survey.

First, [Figure 5](#) plots the filtered probability for each policy state. Blue is the dominant state: it covers most of the space from December 2012 to September 2015 and from December 2016 to the end of the sample, which constitutes 70% of the ELB period. In this state, the yield curve is basically flat (see the blue line in the right panel of [Figure 3](#)). The remainder of the sample is mainly in yellow and purple. The probability of the purple state peaked twice in November 2015 and February 2016, which are the months before the ECB lowered the deposit rate to -0.3% and -0.4%, respectively. The purple area corresponds to the purple line in the right panel of [Figure 3](#), and the yield curve is downward sloping. The yellow

state corresponds to the yellow line in Figure 3, where the yield curve is initially flat, and then slope downwards. This state indicates agents do not expect the central bank to cut rates in the next month. However, they do expect future policy actions. The yellow area dominates between July and November in 2012, and from March to November in 2016. The least prominent state is in red, which implies agents expect the central bank to make an immediate cut, but they also think this cut is the last one in the history. This scenario appears less plausible.

Figure 6: Probability of rate cut

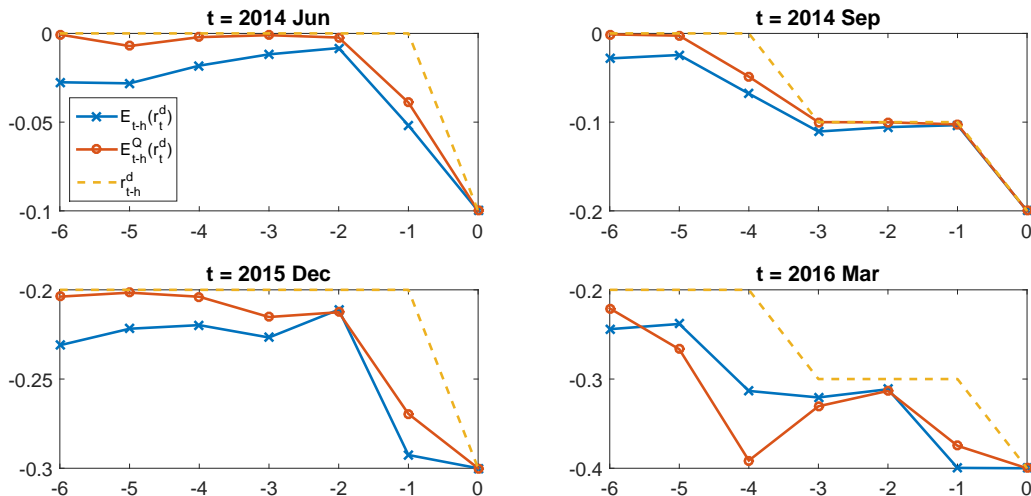


Notes: Red crosses: time  $t - 1$  probability of rate cut for month  $t$  from our model:  $\mathbb{P}_{t-1}(r_t^d = r_{t-1}^d - 0.1) = \alpha_{1,\Delta_{t-1}=0} \times \mathbb{P}_{t-1}(\Delta_{t-1} = 0) + \alpha_{1,\Delta_{t-1}=1} \times \mathbb{P}_{t-1}(\Delta_{t-1} = 1)$ . Black circles: Bloomberg survey expectation, measured as the fraction of respondents that expect a cut. Blue bars: the four rate cuts in June 2014, September 2014, December 2015, and March 2016. X-axis: time. Y-axis: probability.

Next, we compute the one-month ahead probability of a cut on the policy rate from our model and compare it with the Bloomberg survey which is conducted one week before the central bank's scheduled meetings. Figure 6 plots the four actual cuts in blue vertical bars together with our model predictions in red crosses and the Bloomberg survey expectations in black dots. On June 5, 2014, the ECB cuts the rate from 0 to -0.1% for the first time. In May, our model predicts this event with more than 50% probability. As a comparison, over 90% of the respondents of the Blomberg survey expected the cut. The second cut in

September 2014 was a surprise to both economists and the market. The next two cuts from -0.2% to -0.3%, and then subsequently to -0.4%, were largely anticipated. For the rest of the meetings, market participants do not price in much probability of an immediate cut. This exercise confirms market participants' expectations are consistent with economists' views.

Figure 7: Expected deposit facility rate



Notes: Blue lines with crosses are  $\mathbb{E}_{t-h}(r_t^d)$ ; red lines with circles are  $\mathbb{E}_{t-h}^Q(r_t^d)$ ; yellow dashed lines are  $r_{t-h}^d$ .  $t =$  June 2014 (top left), September 2014 (top right), December 2015 (bottom left), and March 2016 (bottom right). X-axis:  $-h$ , Y-axis: annualized interest rates in percentage points.

The Bloomberg survey is conducted one week before each meeting. The yield curve, however, contains richer information and further into the future. In Figure 7, we further inspect for how long the market has anticipated some of the developments. It plots the market's expectations  $h$  months before the four event dates for  $h = 0, 1, 2, \dots, 6$ . The blue lines with crosses are the physical expectations  $\mathbb{E}_{t-h}(r_t^d)$ , the red lines with circles are the risk-neutral expectations  $\mathbb{E}_{t-h}^Q(r_t^d)$ , and the then deposit rates  $r_{t-h}^d$  are in yellow dashed lines. The difference between the blue or red and the yellow lines captures an anticipated rate cut. For now, we focus on the risk-neutral expectations (in red), because the yield curve pins them down more accurately. We will return to the difference between the physical and risk-neutral expectations in Subsection 6.2.

Consistent with [Figure 6](#), the June 2014 and December 2015 cuts were anticipated one month ahead, whereas the September 2014 cut was completely unanticipated. The most interesting case is March 2016. Under the risk-neutral expectation, a cut to  $-0.4\%$  was expected 4 months before, when the actual rate was  $-0.2\%$ . Then agents revised up their expectations for the next two months. Eventually, when  $h = 1$ , agents fully priced in the  $-0.4\%$  for the next month.

## 6 NIRP’s impact on the yield curve

### 6.1 Policy analyses

Assessing the impact of the NIRP is of great interest to both academia and policy makers, and is one main goal of the paper. Different from the existing literature<sup>5</sup>, we focus on the NIRP’s passthrough to interest rates, which operates as the main channel for monetary policy to affect the macroeconomy.

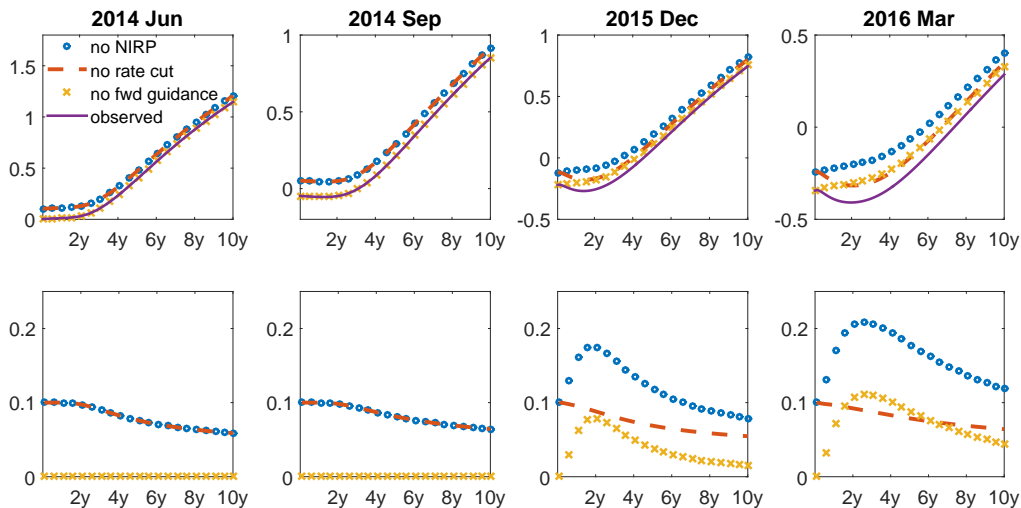
We are interested in the the following question: what would have happened if the ECB had not cut the deposit rate or provided any forward guidance to markets? Specifically, we examine how the yield curve would have behaved if the deposit rate was unchanged from the previous month and both  $\Delta$  and  $\Delta^l$  were at state 0 on the four days when the ECB lowered the deposit rate by 10 basis points.

We plot the results of the experiment in [Figure 8](#). The upper panels plot counterfactual (in blue circles) and observed (in purple lines) yield curves, while the lower panels plot their differences in blue circles. For all four dates, the short end of the yield curve would have been 10 basis points higher if it were not for the expansionary policy. However, the NIRP had different impacts in the medium run. For June and September 2014, the differences between the counterfactual and observed yield curves are downward sloping, whereas those

---

<sup>5</sup>Much of the existing literature has focused on whether and how much the NIRP has affected banks’ profitability; see, for example, Borio et al. (2015), Jobst and Lin (2016), and Cœuré (2016).

Figure 8: Policy analyses



*Notes:* Upper panel: counterfactual and observed yield curves; lower panel: differences between counterfactual and observed yield curves. Blue circles: counterfactual without negative interest rate policy; red dashed lines: counterfactual without rate cuts; yellow crosses: counterfactual without forward guidance; purple lines: observed yield curves as fitted by our model. X-axis: maturity. Y-axis: annualized interest rates in percentage points.

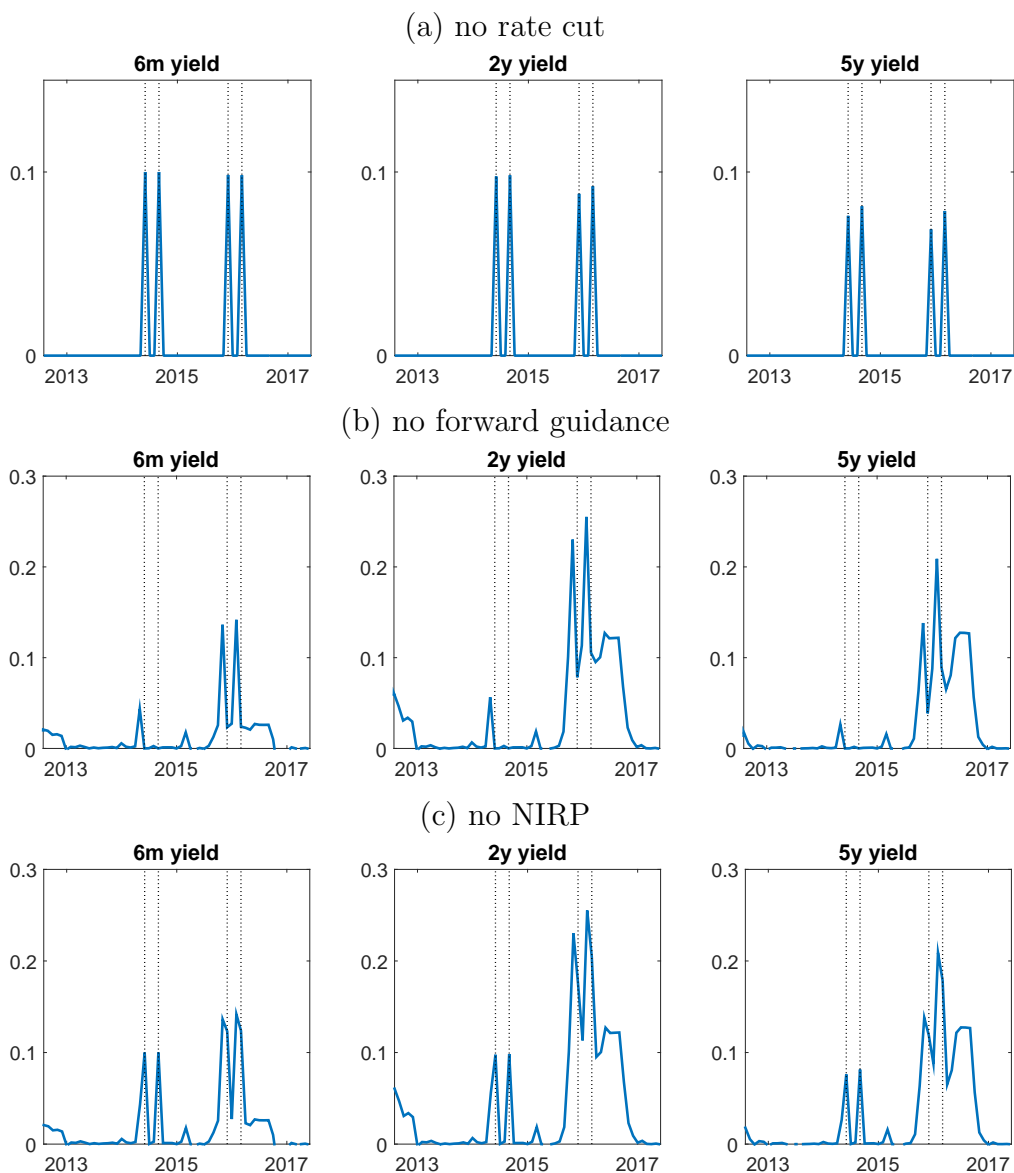
for December 2015 and March 2016 have a humped shape.

To better understand this difference, we perform further experiments to decompose the impact of a rate cut from that of forward guidance. First, we assume that the deposit rate did not change, and plot it in red dashed lines. If the deposit rate were not cut, short-term interest rates would have been about 10 basis points higher. Long-term interest rates would also have been higher but by less amount. That is because the deposit rate is less relevant for longer horizons, where the probability for the lower bound to bind becomes smaller.

In the second experiment, we assume that both  $\Delta$  and  $\Delta^l$  were 0, and plot it in yellow crosses. Forward guidance did not have any impact on the first two dates, implying markets did not price in any future cuts. In contrast, on the last two dates, forward guidance had a sizable impact, mainly in the middle section. Specifically, markets expect further easing, lowering the two-year rate by about 10 basis points.

The NIRP has a broader impact on the yield curve than just the four event dates. [Figure 9](#)

Figure 9: Policy analyses - time series



*Notes:* Difference between counterfactual yields and observed yields for 6m, 2y and 5y maturities. Upper panel: counterfactual with no rate cut; middle panel: counterfactual with no forward guidance; lower panel: counterfactual with no negative interest rate policy. Vertical dashed bars: four event dates. X-axis: time. Y-axis: annualized interest rates in percentage points.

provides a complete picture of the NIRP over the entire ELB period. We plot the difference between counterfactual and observed interest rates over time for short, medium, and long maturities. The top, middle, and bottom panels correspond to counterfactuals where the policy rate were not cut, forward guidance were absent, and both. From the top panels, the impact of rate cut shows up only on the four dates studied in [Figure 8](#), and it is more prominent on the short end. Intuitively, forward guidance lowered the yield curve the month before the first, third and fourth cuts. For the first one, it disappeared on the month of the actual cut. However, for the last two event dates, forward guidance prevailed even when and after the cut was realized, and it continued to put downward pressure on yields till late 2016. Forward guidance also lowered the yield curve at the beginning of the sample in 2013. Across different maturities, forward guidance has the most influence on medium-term interest rates, 2-year rate for example. The NIRP constitutes both rate cut and forward guidance.

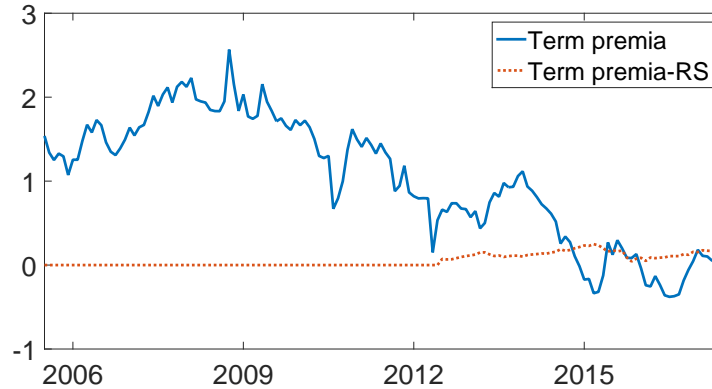
## 6.2 Risk premium

In [Figure 7](#), there is a wedge between the physical (in blue) and risk-neutral (in red) expectations of the deposit rate, which introduces a risk premium. Most of the time, risk-neutral expectations are above or very close to physical expectations, reflecting a positive or near zero risk premium. The intuition for this result is that risk-averse agents put more weight on the bad state of the economy in the risk-neutral measure. Typically, agents associate a rate cut with an expansionary monetary policy, which they expect to stimulate the economy. Hence, we see higher risk-neutral expectations than their physical counterparts.

One prominent and interesting exception happened four months before March 2016, when the difference between the risk-neutral and physical expectations was negative and reached almost -10 basis points. In this case, economic agents might have taken a potential cut in March 2016 as a sign of a weak economy, and hence put more weight into this “bad” economic state.

A related concept is the term premium, which is one of the focal points for the term

Figure 10: 10-year term premium



*Notes:* Blue solid line: 10-year term premium from our main model; red dashed line: the regime-switching portion of term premium. X-axis: time; Y-axis: interest rates in percentage points. Sample spans from July 2005 to June 2017.

structure literature.<sup>6</sup> We plot the time series of the 10-year yield term premium for the Euro area from our model in Figure 10. The overall term premium is in the blue solid line, and that associated with the time variation of the deposit rate in the red dashed line. The red line is positive and in the order of magnitude of 0.1%, which is consistent with what we find in Figure 7.

The overall term premium has trended down since 2009. At the ELB, we observe some negative term premia. This observation can mainly be attributed to the QE programs, which purchase longer-term government bonds and reduce yields through the term premium channel.<sup>7</sup>

## 7 Model comparison

Table 2 compares our model with several alternatives in terms of log likelihood values and measurement errors. The first column is our main model specification. The second column is our model without the  $\Delta_t^l$  state. Columns 3 to 5 are benchmark SRTSMs in the literature,

<sup>6</sup>See, for example, Duffee (2002), Wright (2011), Bauer et al. (2012, 2014), and Creal and Wu (2016).

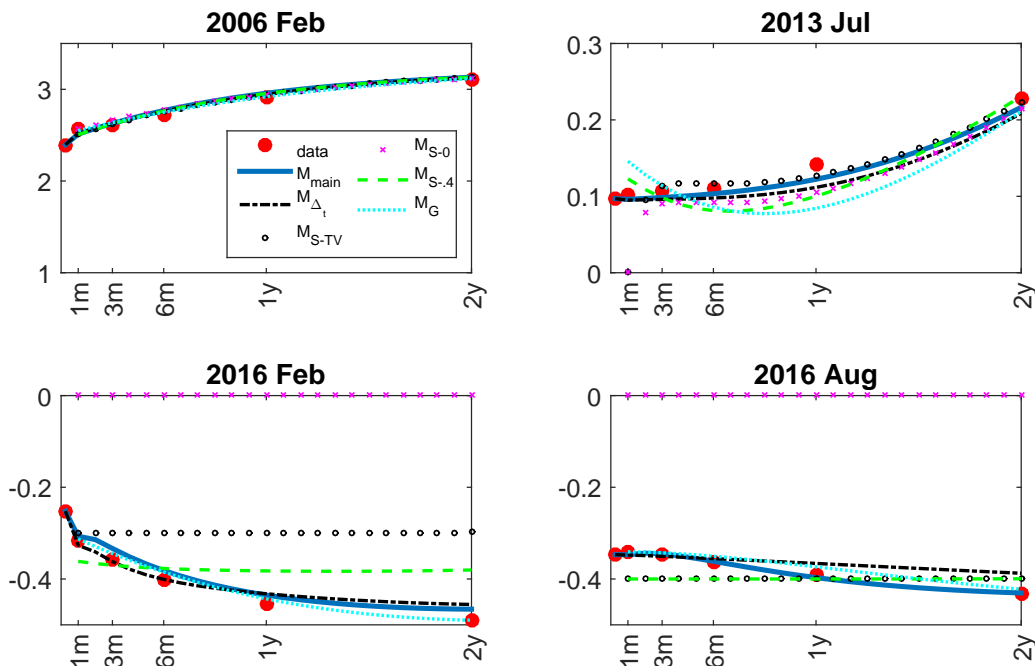
<sup>7</sup>This channel has been discussed in Gagnon et al. (2011), Krishnamurthy and Vissing-Jorgensen (2011), Hamilton and Wu (2012a), Wu and Zhang (2017), and Wu and Zhang (2018).

Table 2: Model comparison

		$M_{main}$	$M_{\Delta_t}$	$M_{S-TV}$	$M_{S-0}$	$M_{S-.4}$	$M_G$
full sample	log likelihood	<b>935.48</b>	911.94	709.55	279.12	663.46	603.32
	(n,m)	Measurement errors of $f_{nmt}$					
	(0,1)	<b>3.62</b>	4.11	8.01	14.32	4.13	5.50
	(3,3)	<b>6.20</b>	6.51	6.39	16.04	6.61	7.38
	(6,6)	<b>5.83</b>	6.66	6.72	16.70	6.39	9.06
	(12,12)	6.24	6.48	6.81	16.21	6.96	<b>5.91</b>
	(24,12)	<b>8.75</b>	8.92	9.33	15.14	10.63	11.10
	(60,12)	8.25	8.47	<b>8.24</b>	9.34	8.29	8.44
	(84,12)	5.05	<b>4.94</b>	4.96	6.18	5.63	5.79
	(108,12)	8.17	8.20	<b>8.13</b>	9.01	9.22	8.77
ELB	(n,m)	Measurement errors of $f_{nmt}$					
	(0,1)	1.42	<b>1.35</b>	10.67	20.89	3.55	3.98
	(3,3)	<b>3.64</b>	3.93	3.97	22.44	5.00	4.41
	(6,6)	<b>3.87</b>	4.83	5.08	23.52	4.57	6.56
	(12,12)	3.40	4.38	5.52	22.66	5.54	<b>1.91</b>
	(24,12)	<b>4.59</b>	4.89	6.67	18.71	10.05	9.69
	(60,12)	8.92	9.17	8.97	11.24	<b>8.71</b>	9.16
	(84,12)	<b>4.32</b>	4.74	4.81	6.55	5.22	6.82
	(108,12)	<b>6.92</b>	7.10	7.39	8.36	9.23	9.29

Notes: Top panel: full sample from July 2005 to June 2017; bottom panel: ELB sample from July 2012 to June 2017. First column: our main model  $M_{main}$ ; second column:  $M_{\Delta_t}$  without  $\Delta_t^i$ ; third column: benchmark shadow rate model  $M_{S-TV}$  with myopic agents and time-varying lower bound equal to the deposit rate; fourth column: benchmark shadow rate model  $M_{S-0}$  with a constant lower bound at zero; fifth column: benchmark shadow rate model  $M_{S-.4}$  with a constant lower bound at -0.4%; sixth column: benchmark GATSM. Measurement errors are in basis points, and computed as the root-mean-square errors between observed and model-implied short rates and forward rates. Forward rate  $f_{nmt}$  is the forward contract from  $t+n$  to  $t+n+m$ . We highlight the smallest measurement errors, and the highest log likelihood value.

Figure 11: Fitted yield curves



*Notes:* Red dots: observed yields; blue solid line: our main model  $M_{main}$ ; black dash-dotted line:  $M_{\Delta_t}$  without  $\Delta_t^l$ ; black circles: benchmark model  $M_{BM-TV}$  with exogenously varying lower bound; pink cross: benchmark model  $M_{BM-0}$  with a constant lower bound at zero; green dashed line: benchmark model  $M_{BM-.4}$  with a constant lower bound at -0.4%; light blue dotted line: GATSM  $M_G$ . X-axis: maturity; Y-axis: interest rates in percentage points. Top left panel: February 2006; top right panel: July 2013; bottom left: February 2016; bottom right: July 2016.

and the corresponding lower bounds are specified as the current deposit rate, 0, and -0.4%, respectively. Note, agents are not forward looking in terms of the lower bound in these existing SRTSMs. The last column is the GATSM. See details in [Appendix C](#).

Our main model has the highest likelihood value, and provides the best overall fit to the forward curve with smaller measurement errors. All the evidence points to the conclusion that the data favor our main model over these alternative model specifications.

[Figure 11](#) provides some visual evidence by comparing the observed data in red dots with yield curves implied by various models. When the ELB was not binding (see the top left panel), all models fit the data similarly well. When the yield curve has a flat short end at the beginning of the ELB (see the top right panel), our main model and  $M_{\Delta_t}$  provide a better

fit than other models. In theory, the existing shadow rate models  $M_{S-TV}$ ,  $M_{S-0}$ , and  $M_{S-.4}$  should be able to fit this pattern. But in practice, because they ignore the spread between the deposit rate and EONIA, discrepancies appear at the very short end. The GATSM is expected to perform poorly in this case, which is what motivates the entire literature on the SRTSM. Not able to fit the flat short end of the yield curve makes the GATSM one of the worst models; see [Table 2](#).

In the bottom panels, none of the SRTSMs existing in the literature are able to generate a downward sloping short end to mimic the data when the NIRP is in play. Intuitively, agents in these models are myopic, and do not expect further development of the policy rate. Both our main model and  $M_{\Delta_t}$  are able to generate a downward slope through agents' expectations that the future deposit rate might further decrease. However,  $M_{\Delta_t}$  is not flexible enough to match the data for both February and August 2016. Our main model, which is motivated by various shapes of the yield curve in [Figure 1](#), fits all the dates well.

## 8 Conclusion

We have proposed a new shadow rate term structure model that captures the NIRP in the Euro area. We model the discrete movement of the deposit rate with a simple and intuitive regime-switching model. To capture various shapes in the short end of the yield curve, we introduce two latent state variables: one for the immediate monetary policy stance, and the other for future stance in longer horizons. We illustrate that the two do not always coincide, and therefore, it is useful to have both of the indicators. Compared to alternative models, including several SRTSMs proposed in the literature, and the GATSM, our new model fits the data the best.

We use our model to extract the market's expectations on the NIRP. Overall, expectations of financial market participants from our model agree with economists' expectations of the Bloomberg survey. Our model has the advantage over the Bloomberg survey because we can

extract the market's expectations further into the future, whereas the Bloomberg surveys are collected only one week before meetings for monetary policy. We find the June 2014 and December 2015 cuts were expected the month before, and the September 2014 cut was entirely unanticipated. Most interestingly, the March 2016 cut was expected 4 months before the actual cut.

We then evaluate the NIRP's impact on the yield curve with counterfactual policy analyses. The NIRP lowered the short end of the yield curve by 10 basis points on all four days when ECB lowered the deposit rate. The impact decreased with maturity for the first two dates. It featured a humped shape for the last two dates. Specifically, the biggest changes happened for interest rates with maturities around 2 years, which would have been around 20 basis points higher if it were not for the NIRP actions.

We also measure the risk premium associated with the NIRP. We find most of the time, this risk premium is positive or close to zero, which means agents typically associate a rate cut with an expansionary monetary policy. One exception is four months before the March 2016 cut, when the difference between the risk-neutral and physical expectations was almost -10 basis points. Our interpretation is that agents took a potential cut in March 2016 as a sign of weak economic outlook. Relatedly, the NIRP also drives a small but positive term premium on the 10-year yield.

## References

- Adrian, Tobias, Richard K. Crump, and Emanuel Moench**, “Pricing the term structure with linear regressions.,” 2012, *110* (1), 110–138.
- Ang, Andrew and Geert Bekaert**, “Regime Switches in Interest Rates,” *Journal of Business & Economic Statistics*, 2002, *20* (2), 163–182.
- and **Monika Piazzesi**, “A No-Arbitrage Vector Autoregression of Term Structure Dynamics with Macroeconomic and Latent Variables,” *Journal of Monetary Economics*, 2003, *50*, 745–787.
- Bansal, Ravi and Hao Zhou**, “Term structure of interest rates with regime shifts,” *The Journal of Finance*, 2002, *57* (5), 1997–2043.
- Bauer, Michael D. and Glenn D. Rudebusch**, “Monetary Policy Expectations at the Zero Lower Bound,” *Journal of Money, Credit and Banking*, 2016, *48* (7), 1439–1465.
- , – , and **Jing Cynthia Wu**, “Correcting Estimation Bias in Dynamic Term Structure Models,” *Journal of Business & Economic Statistics*, 2012, *30* (3), 454–467.
- , – , and – , “Term Premia and Inflation Uncertainty: Empirical Evidence from an International Panel Dataset: Comment,” *American Economic Review*, January 2014, *104* (1), 323–37.
- Black, Fischer**, “Interest Rates as Options,” *Journal of Finance*, 1995, *50*, 1371–1376.
- Borio, Claudio EV, Leonardo Gambacorta, and Boris Hofmann**, “The Influence of Monetary Policy on Bank Profitability,” 2015. BIS working paper.
- Christensen, J. H. E. and Glenn D. Rudebusch**, “Estimating shadow-rate term structure models with near-zero yields,” *Journal of Financial Econometrics*, 2014, *0*, 1–34.

- Christensen, Jens H.E., Francis X. Diebold, and Glenn D. Rudebusch**, “The affine arbitrage-free class of Nelson-Siegel term structure models.,” 2011, *164* (1), 4–20.
- Cœuré, Benoît**, “Assessing the implications of negative interest rates,” in “speech at the Yale Financial Crisis Forum, Yale School of Management, New Haven,” Vol. 28 2016.
- Creal, Drew D. and Jing Cynthia Wu**, “Estimation of affine term structure models with spanned or unspanned stochastic volatility,” *Journal of Econometrics*, 2015, *185* (1), 60 – 81.
- **and** – , “Bond risk premia in consumption based models.,” 2016. Working paper, University of Chicago, Booth School of Business.
- Dai, Qiang, Kenneth J Singleton, and Wei Yang**, “Regime shifts in a dynamic term structure model of US treasury bond yields,” *Review of Financial Studies*, 2007, *20* (5), 1669–1706.
- de Los Rios, Antonio Diez**, “A New Linear Estimator for Gaussian Dynamic Term Structure Models,” *Journal of Business & Economic Statistics*, 2015, *33* (2), 282–295.
- Duffee, Gregory R.**, “Term premia and interest rate forecasts in affine models,” 2002, *57* (1), 405–443.
- Gagnon, Joseph, Matthew Raskin, Julie Remache, and Brian Sack**, “The Financial Market Effects of the Federal Reserve’s Large-Scale Asset Purchase,” *International Journal of Central Banking*, 2011, *7*, 3–43.
- Hamilton, James D.**, “A New Approach to the Economic Analysis of Nonstationary Time Series and the Business Cycle,” *Econometrica*, 1989, *57* (2), 357–384.
- , *Time Series Analysis*, Princeton, New Jersey: Princeton University Press, 1994.
- **and Jing Cynthia Wu**, “The effectiveness of alternative monetary policy tools in a zero lower bound environment,” 2012, *44* (s1), 3–46.

- **and** –, “Identification and estimation of Gaussian affine term structure models.,” 2012, *168* (2), 315–331.
- **and** –, “Testable Implications of Affine Term Structure Models,” *Journal of Econometrics*, 2014, *178*, 231–242.
- Ichiue, Hibiki and Yoichi Ueno**, “Estimating Term Premia at the Zero Bound : an Analysis of Japanese, US, and UK Yields,” 2013. Bank of Japan Working Paper.
- Jobst, Andreas and Huidan Lin**, “Negative Interest Rate Policy (NIRP): Implications for Monetary Transmission and Bank Profitability in the Euro Area,” 2016. IMF working paper.
- Joslin, Scott, Kenneth J. Singleton, and Haoxiang Zhu**, “A new perspective on Gaussian affine term structure models,” 2011, *27*, 926–970.
- Kim, Chang-Jin**, “Dynamic linear models with Markov-switching,” *Journal of Econometrics*, 1994, *60* (1-2), 1–22.
- Kim, Don H. and Kenneth J. Singleton**, “Term Structure Models and the Zero Bound: an Empirical Investigation of Japanese Yields,” *Journal of Econometrics*, 2012, *170*, 32–49.
- Kortela, Tomi**, “A shadow rate model with time-varying lower bound of interest rates,” 2016. Bank of Finland Research Discussion Paper.
- Krippner, Leo**, “A Tractable Framework for Zero Lower Bound Gaussian Term Structure Models,” August 2013. Australian National University CAMA Working Paper 49/2013.
- Krishnamurthy, Arvind and Annette Vissing-Jorgensen**, “The Effects of Quantitative Easing on Interest Rates: Channels and Implications for Policy,” *Brookings Papers on Economic Activity*, 2011, *2*, 215–265.
- Lemke, Wolfgang and Andreea L Vladu**, “Below the zero lower bound: A shadow-rate term structure model for the euro area,” 2016. Deutsche Bundesbank Discussion Paper.

- Piazzesi, Monika**, “Bond yields and the Federal Reserve,” *Journal of Political Economy*, 2005, *113* (2), 311–344.
- Renne, Jean-Paul**, “A model of the euro-area yield curve with discrete policy rates,” *Studies in Nonlinear Dynamics & Econometrics*, 2012.
- Rudebusch, Glenn D**, “Federal Reserve interest rate targeting, rational expectations, and the term structure,” *Journal of monetary Economics*, 1995, *35* (2), 245–274.
- Wright, J. H.**, “Term Premia and Inflation Uncertainty: Empirical Evidence from an International Panel Dataset,” *American Economic Review*, 2011, *101*, 1514–1534.
- Wu, Jing Cynthia and Fan Dora Xia**, “Measuring the macroeconomic impact of monetary policy at the zero lower bound,” *Journal of Money, Credit and Banking*, 2016, *48* (2-3), 253–291.
- **and** –, “Time-varying lower bound of interest rates in Europe,” 2017. Working paper, University of Chicago, Booth School of Business.
- **and Ji Zhang**, “A Shadow Rate New Keynesian Model,” 2017. NBER Working Paper No. 22856.
- **and** –, “Global Effective Lower Bound and Unconventional Monetary Policy,” 2018. NBER Working Paper No. 24714.

## Appendix A Deriving pricing formula

As shown in Wu and Xia (2016), the forward rate is

$$f_{nt} \approx \mathbb{E}_t^{\mathbb{Q}}[r_{t+n}] - \frac{1}{2} \left( \text{Var}_t^{\mathbb{Q}} \left[ \sum_{j=1}^n r_{t+j} \right] - \text{Var}_t^{\mathbb{Q}} \left[ \sum_{j=1}^{n-1} r_{t+j} \right] \right). \quad (\text{A.1})$$

### Appendix A.1 Model with $\underline{r}_{t+n}$

Wu and Xia (2016) show (A.1) can be further approximated:

$$f_{nt} \approx \mathbb{E}_t^{\mathbb{Q}}[\max(s_{t+n}, \underline{r}_{t+n})] - \mathbb{Q}_t(s_{t+n} \geq \underline{r}_{t+n}) \times \frac{1}{2} \left( \text{Var}_t^{\mathbb{Q}} \left[ \sum_{j=1}^n s_{t+j} \right] - \text{Var}_t^{\mathbb{Q}} \left[ \sum_{j=1}^{n-1} s_{t+j} \right] \right).$$

The right-hand side equals

$$\begin{aligned} & \sum_{\underline{r}_{t+n}} \left[ -\mathbb{Q}_t(s_{t+n} \geq \underline{r}_{t+n} | \underline{r}_{t+n}) \times \frac{1}{2} \left( \text{Var}_t^{\mathbb{Q}} \left[ \sum_{j=1}^n s_{t+j} \right] - \text{Var}_t^{\mathbb{Q}} \left[ \sum_{j=1}^{n-1} s_{t+j} \right] \right) \right. \\ & \left. + \mathbb{E}_t^{\mathbb{Q}}[\max(s_{t+n}, \underline{r}_{t+n} | \underline{r}_{t+n})] \right] \mathbb{Q}_t(\underline{r}_{t+n}). \end{aligned}$$

According to Wu and Xia (2016), the expression inside the sum conditioning on the lower bound equals

$$\underline{r}_{t+n} + \sigma_n^{\mathbb{Q}} g \left( \frac{a_n + b'_n X_t - \underline{r}_{t+n}}{\sigma_n^{\mathbb{Q}}} \right).$$

Hence, we obtain (3.10).

### Appendix A.2 Model with $\underline{r}_{t+n}$ and $sp_{t+n}$

First,

$$\mathbb{Q}_t(s_{t+n} - sp_{t+n}) \sim N(\bar{a}_n + b'_n X_t - c_n - d_n sp_t, (\tilde{\sigma}_n^{\mathbb{Q}})^2),$$

where  $\bar{a}_n \equiv \delta_0 + \delta'_1 \left( \sum_{j=0}^{n-1} (\rho^{\mathbb{Q}})^j \right) \mu^{\mathbb{Q}}$ . The first term on the right-hand side of (A.1) is

$$\begin{aligned} \mathbb{E}_t^{\mathbb{Q}}[r_{t+n}] &= \mathbb{E}_t^{\mathbb{Q}}[\max(\underline{r}_{t+n} + sp_{t+n}, s_{t+n})] \\ &= \mathbb{E}_t^{\mathbb{Q}}[\max(\underline{r}_{t+n}, s_{t+n} - sp_{t+n}) + sp_{t+n}] \\ &= \sum_{\underline{r}_{t+n}} \mathbb{Q}_t(\underline{r}_{t+n}) \mathbb{E}_t^{\mathbb{Q}}[\max(\underline{r}_{t+n}, s_{t+n} - sp_{t+n}) | \underline{r}_{t+n}] + \mathbb{E}_t^{\mathbb{Q}}(sp_{t+n}) \\ &= \sum_{\underline{r}_{t+n}} \mathbb{Q}_t(\underline{r}_{t+n}) \left( \underline{r}_{t+n} + \tilde{\sigma}_n^{\mathbb{Q}} g \left( \frac{\bar{a}_n + b'_n X_t - c_n - d_n sp_t - \underline{r}_{t+n}}{\tilde{\sigma}_n^{\mathbb{Q}}} \right) \right) + c_n + d_n sp_t, \end{aligned}$$

where the derivation for the last equal sign follows Wu and Xia (2016).

The second term of (A.1) is

$$\begin{aligned}
& \frac{1}{2} \left( \text{Var}_t^{\mathbb{Q}} \left[ \sum_{j=1}^n r_{t+j} \right] - \text{Var}_t^{\mathbb{Q}} \left[ \sum_{j=1}^{n-1} r_{t+j} \right] \right) \\
& \approx \mathbb{Q}_t(s_{t+n} - sp_{t+n} \geq r_{t+n}) \times \frac{1}{2} \left( \text{Var}_t^{\mathbb{Q}} \left[ \sum_{j=1}^n s_{t+j} \right] - \text{Var}_t^{\mathbb{Q}} \left[ \sum_{j=1}^{n-1} s_{t+j} \right] \right) \\
& = \sum_{r_{t+n}} \mathbb{Q}_t(r_{t+n}) \mathbb{Q}_t(s_{t+n} - sp_{t+n} \geq r_{t+n} | r_{t+n}) \times \frac{1}{2} \left( \text{Var}_t^{\mathbb{Q}} \left[ \sum_{j=1}^n s_{t+j} \right] - \text{Var}_t^{\mathbb{Q}} \left[ \sum_{j=1}^{n-1} s_{t+j} \right] \right) \\
& = \sum_{r_{t+n}} \mathbb{Q}_t(r_{t+n}) \Phi \left( \frac{\bar{a}_n + b'_n X_t - c_n - d_n sp_t - r_{t+n}}{\tilde{\sigma}_n^{\mathbb{Q}}} \right) \times (\bar{a}_n - a_n),
\end{aligned}$$

where the first approximation sign and last equal sign follow Wu and Xia (2016).

Adding them together yields (4.2):

$$\begin{aligned}
f_{nt} & \approx \sum_{r_{t+n}} \mathbb{Q}_t(r_{t+n}) \left( r_{t+n} + \tilde{\sigma}_n^{\mathbb{Q}} g \left( \frac{a_n + b'_n X_t - c_n - d_n sp_t - r_{t+n}}{\tilde{\sigma}_n^{\mathbb{Q}}} \right) \right) + c_n + d_n sp_t \\
& = \sum_{r_{t+n}} \mathbb{Q}_t(r_{t+n}) \left( r_{t+n} + c_n + d_n sp_t + \tilde{\sigma}_n^{\mathbb{Q}} g \left( \frac{a_n + b'_n X_t - c_n - d_n sp_t - r_{t+n}}{\tilde{\sigma}_n^{\mathbb{Q}}} \right) \right),
\end{aligned}$$

where the approximation follows Wu and Xia (2016).

## Appendix B Estimation

We adapt the algorithm of Kim (1994) to our model by incorporating the extended Kalman filter. Stack the observation equation in (4.6) for all maturities together with (4.5):

$$F_t^o = F(X_t, sp_t, r_t^d, \Xi_t) + \tilde{\eta}_t, \text{ where } \tilde{\eta}_t \sim N(0, \omega^2 I_8).$$

Define  $\mathcal{Y}_t \equiv \{F_{1:t}^o, r_{1:t}^d, sp_{1:t}\}$ , and  $\Xi_t \equiv \{\Delta_t, \Delta_t^l\}$ .

**Step 1:** Approximate the conditional distribution of  $X_t$  with  $X_t | \Xi_t, \mathcal{Y}_t \sim N(\hat{X}_{t|t}^{\Xi_t}, P_{t|t}^{\Xi_t})$ . We initialize  $\hat{X}_{0|0}^{s_0} = (I_3 - \rho)^{-1} \mu$ ,  $vec(P_{0|0}^{s_0}) = (I_9 - (\rho \otimes \rho))^{-1} vec(\Sigma \Sigma')$ , and  $\mathbb{P}(s_0)$  follows a discrete uniform distribution.

We apply the extended Kalman filter as follows:

$$\hat{X}_{t+1|t}^{\Xi_{t+1}, \Xi_t} = \mu + \rho \hat{X}_{t|t}^{\Xi_t}, \quad (\text{B.1})$$

$$P_{t+1|t}^{\Xi_{t+1}, \Xi_t} = \rho P_{t|t}^{\Xi_t} \rho' + \Sigma \Sigma', \quad (\text{B.2})$$

$$\hat{\eta}_{t+1|t}^{\Xi_{t+1}, \Xi_t} = F_{t+1}^o - F(\hat{X}_{t+1|t}^{\Xi_{t+1}, \Xi_t}, sp_{t+1}, r_{t+1}^d, \Xi_{t+1}), \quad (\text{B.3})$$

$$H_{t+1|t}^{\Xi_{t+1}, \Xi_t} = \left( \frac{\partial F(X_{t+1}, sp_{t+1}, r_{t+1}^d, \Xi_{t+1})}{\partial X'_{t+1}} \Big|_{X_{t+1} = \hat{X}_{t+1|t}^{\Xi_{t+1}, \Xi_t}} \right)', \quad (\text{B.4})$$

$$K_{t+1|t}^{\Xi_{t+1}, \Xi_t} = P_{t+1|t}^{\Xi_{t+1}, \Xi_t} H_{t+1|t}^{\Xi_{t+1}, \Xi_t} \left( (H_{t+1|t}^{\Xi_{t+1}, \Xi_t})' P_{t+1|t}^{\Xi_{t+1}, \Xi_t} H_{t+1|t}^{\Xi_{t+1}, \Xi_t} + \omega I_8 \right)^{-1}, \quad (\text{B.5})$$

$$\hat{X}_{t+1|t+1}^{\Xi_{t+1}, \Xi_t} = \hat{X}_{t+1|t}^{\Xi_{t+1}, \Xi_t} + K_{t+1|t}^{\Xi_{t+1}, \Xi_t} \hat{\eta}_{t+1|t}^{\Xi_{t+1}, \Xi_t}, \quad (\text{B.6})$$

$$P_{t+1|t+1}^{\Xi_{t+1}, \Xi_t} = \left( I_3 - K_{t+1|t}^{\Xi_{t+1}, \Xi_t} (H_{t+1|t}^{\Xi_{t+1}, \Xi_t})' \right) P_{t+1|t}^{\Xi_{t+1}, \Xi_t}. \quad (\text{B.7})$$

Note we will write out  $X_{t+1|t+1}^{\Xi_{t+1}}$  and  $P_{t+1|t+1}^{\Xi_{t+1}}$  in terms of  $X_{t+1|t+1}^{\Xi_{t+1}, \Xi_t}$  and  $P_{t+1|t+1}^{\Xi_{t+1}, \Xi_t}$  in Step 3 to complete the iteration. The likelihood for bond prices at  $t + 1$  is

$$\begin{aligned} & \mathbb{P}(F_{t+1}^o | r_{t+1}^d, sp_{t+1}, \mathcal{Y}_t, \Xi_{t+1}, \Xi_t) \\ &= \left( 2\pi \left| (H_{t+1|t}^{\Xi_{t+1}, \Xi_t})' P_{t+1|t}^{\Xi_{t+1}, \Xi_t} H_{t+1|t}^{\Xi_{t+1}, \Xi_t} + \omega I_8 \right| \right)^{-1/2} \\ & \exp \left( -\frac{1}{2} (\hat{\eta}_{t+1|t}^{\Xi_{t+1}, \Xi_t})' \left| (H_{t+1|t}^{\Xi_{t+1}, \Xi_t})' P_{t+1|t}^{\Xi_{t+1}, \Xi_t} H_{t+1|t}^{\Xi_{t+1}, \Xi_t} + \omega I_8 \right|^{-1} \hat{\eta}_{t+1|t}^{\Xi_{t+1}, \Xi_t} \right). \end{aligned} \quad (\text{B.8})$$

**Step 2:** We compute the distribution  $\mathbb{P}(\Xi_{t+1}, |\mathcal{Y}_{t+1})$  as follows:

$$\mathbb{P}(\Xi_{t+1} | \mathcal{Y}_{t+1}) = \sum_{\Xi_t} \mathbb{P}(\Xi_{t+1}, \Xi_t | \mathcal{Y}_{t+1}), \quad (\text{B.9})$$

where

$$\begin{aligned} \mathbb{P}(\Xi_{t+1}, \Xi_t | \mathcal{Y}_{t+1}) &= \frac{\mathbb{P}(F_{t+1}^o, r_{t+1}^d, sp_{t+1}, \Xi_{t+1}, \Xi_t | \mathcal{Y}_t)}{\mathbb{P}(F_{t+1}^o, r_{t+1}^d, sp_{t+1} | \mathcal{Y}_t)} \\ &= \frac{\mathbb{P}(F_{t+1}^o, r_{t+1}^d, sp_{t+1} | \Xi_{t+1}, \Xi_t, \mathcal{Y}_t) \mathbb{P}(\Xi_{t+1}, \Xi_t | \mathcal{Y}_t)}{\mathbb{P}(F_{t+1}^o, r_{t+1}^d, sp_{t+1} | \mathcal{Y}_t)} \\ &= \frac{\mathbb{P}(F_{t+1}^o, r_{t+1}^d, sp_{t+1} | \Xi_{t+1}, \Xi_t, \mathcal{Y}_t) \mathbb{P}(\Xi_{t+1}, \Xi_t | \mathcal{Y}_t)}{\sum_{\Xi_{t+1}, \Xi_t} \mathbb{P}(F_{t+1}^o, r_{t+1}^d, sp_{t+1} | \Xi_{t+1}, \Xi_t, \mathcal{Y}_t) \mathbb{P}(\Xi_{t+1}, \Xi_t | \mathcal{Y}_t)}. \end{aligned} \quad (\text{B.10})$$

We compute  $\mathbb{P}(\Xi_{t+1}, \Xi_t | \mathcal{Y}_t)$  as follows:

$$\begin{aligned} \mathbb{P}(\Xi_{t+1}, \Xi_t | \mathcal{Y}_t) &= \mathbb{P}(\Xi_{t+1} | \Xi_t) \mathbb{P}(\Xi_t | \mathcal{Y}_t) \\ &= \mathbb{P}(\Delta_t | \Delta_{t-1}, \Delta_{t-1}^l) \mathbb{P}(\Delta_t^l | \Delta_{t-1}^l) \mathbb{P}(\Xi_t | \mathcal{Y}_t), \end{aligned} \quad (\text{B.11})$$

where the first two terms are given by the P version of (2.4) and (2.5), respectively. We compute  $\mathbb{P}(F_{t+1}^o, r_{t+1}^d, sp_{t+1} | \mathcal{Y}_t, \Xi_{t+1}, \Xi_t)$  in (B.10) as follows:

$$\begin{aligned} \mathbb{P}(F_{t+1}^o, r_{t+1}^d, sp_{t+1} | \mathcal{Y}_t, \Xi_{t+1}, \Xi_t) &= \mathbb{P}(F_{t+1}^o | r_{t+1}^d, sp_{t+1}, \mathcal{Y}_t, \Xi_{t+1}, \Xi_t) \\ &\quad \mathbb{P}(r_{t+1}^d | sp_{t+1}, \mathcal{Y}_t, \Xi_{t+1}, \Xi_t) \mathbb{P}(sp_{t+1} | \mathcal{Y}_t, \Xi_{t+1}, \Xi_t). \end{aligned} \quad (\text{B.12})$$

The first term in (B.12) is calculated in (B.8). Using (2.2), the second term is

$$\mathbb{P}(r_{t+1}^d | sp_{t+1}, \mathcal{Y}_t, \Xi_{t+1}, \Xi_t) = \mathbb{P}(r_{t+1}^d | r_t^d, \Delta_t) = \mathbf{1}_{\{r_{t+1}^d = r_t^d\}} \times (1 - \alpha_{1, \Delta_t}) + \mathbf{1}_{\{r_{t+1}^d = r_t^d - 0.1\%\}} \times \alpha_{1, \Delta_t}.$$

Using the P version of (4.1), the third term in (B.12) is

$$\mathbb{P}(sp_{t+1} | \mathcal{Y}_t, \Xi_{t+1}, \Xi_t) = \mathbb{P}(sp_{t+1} | sp_t) = (2\pi\sigma_{sp}^2)^{-1/2} \exp\left(-\frac{(sp_{t+1} - \mu_{sp} - \rho_{sp} sp_t)^2}{2\sigma_{sp}^2}\right).$$

With (B.11) and (B.12), we can also calculate the log likelihood for period  $t + 1$

$$\mathbb{P}(F_{t+1}^o, r_{t+1}^d, sp_{t+1} | \mathcal{Y}_t) = \sum_{\Xi_{t+1}, \Xi_t} \mathbb{P}(F_{t+1}^o, r_{t+1}^d, sp_{t+1} | \mathcal{Y}_t, \Xi_{t+1}, \Xi_t) \mathbb{P}(\Xi_{t+1}, \Xi_t | \mathcal{Y}_t). \quad (\text{B.13})$$

**Step 3:** Finally, we can complete the recursion in (B.1) - (B.7) with

$$\begin{aligned} \hat{X}_{t+1|t+1}^{\Xi_{t+1}} &= \frac{\sum_{\Xi_t} \mathbb{P}(\Xi_{t+1}, \Xi_t | \mathcal{Y}_{t+1}) \hat{X}_{t+1|t+1}^{\Xi_{t+1}, \Xi_t}}{\mathbb{P}(\Xi_{t+1} | \mathcal{Y}_{t+1})}, \\ P_{t+1|t+1}^{\Xi_{t+1}} &= \frac{\sum_{\Xi_t} \mathbb{P}(\Xi_{t+1}, \Xi_t | \mathcal{Y}_{t+1}) \left( P_{t+1|t+1}^{\Xi_{t+1}, \Xi_t} + (\hat{X}_{t+1|t+1}^{\Xi_{t+1}} - \hat{X}_{t+1|t+1}^{\Xi_{t+1}, \Xi_t})(\hat{X}_{t+1|t+1}^{\Xi_{t+1}} - \hat{X}_{t+1|t+1}^{\Xi_{t+1}, \Xi_t})' \right)}{\mathbb{P}(\Xi_{t+1} | \mathcal{Y}_{t+1})}, \end{aligned}$$

where  $\hat{X}_{t+1|t+1}^{\Xi_{t+1}, \Xi_t}$  and  $P_{t+1|t+1}^{\Xi_{t+1}, \Xi_t}$  are calculated in (B.6) and (B.7), and  $\mathbb{P}(\Xi_{t+1} | \mathcal{Y}_{t+1})$  is from (B.9).

**Log likelihood** The log likelihood is  $\sum_{t=0}^{T-1} \log(\mathbb{P}(F_{t+1}^o, r_{t+1}^d, sp_{t+1} | \mathcal{Y}_t))$ . At the ELB,  $\mathbb{P}(F_{t+1}^o, r_{t+1}^d, sp_{t+1} | \mathcal{Y}_t)$  is calculated in (B.13). Before the ELB,  $sp_t, r_t^d, \Xi_t$  are all irrelevant, and  $\mathbb{P}(F_{t+1}^o, r_{t+1}^d, sp_{t+1} | \mathcal{Y}_t) = \mathbb{P}(F_{t+1}^o | F_t^o)$ , which is computed by (B.8) through the extended Kalman filter in (B.1) - (B.7) by ignoring  $\Xi_t, \Xi_{t+1}$ .

## Appendix C Alternative models

Table C.1: Model specifications

	short description	full description
$M_{main}$	main model	The main model specified in Sections 2-3.
$M_{\Delta_t}$	model with only $\Delta_t$	Impose $\alpha_{00,\Delta_t^i} = \alpha_{00}, \alpha_{11,\Delta_t^i} = \alpha_{11}, \alpha_{00,\Delta_t^i}^Q = \alpha_{00}^Q, \alpha_{11,\Delta_t^i}^Q = \alpha_{11}^Q$ on our main model.
$M_{S-TV}$	benchmark shadow rate model with time-varying lower bound and myopic agents	$\underline{r}_t = r_t^d$ for ELB. But agents are not forward looking, and think the future lower bound would stay where it is today. Also, $sp_t = 0$ . This specification is similar to Lemke and Vladu (2016), and Kortela (2016).
$M_{S-0}$	benchmark shadow rate model with a constant lower bound at 0	This model has a constant lower bound at 0, and $sp_t = 0$ . This is similar to Christensen and Rudebusch (2014), Wu and Xia (2016), and Bauer and Rudebusch (2016).
$M_{S-.4}$	benchmark shadow rate model with a constant lower bound at -0.4%	This model is the same as the previous one, except the lower bound is changed to -0.4%.
$M_G$	benchmark Gaussian affine term structure model	In this model, $\underline{r}_t = -\infty$ .